Nature of the Ferromagnetic Behavior and Possible Occurrence of the Ferrimagnetic Phase Transition in Genuinely Organic Molecule-Based Assemblages with an $S = 1$ and $S = {}^1/_2$ Antiferromagnetic Alternating Spin Chain: A Green's Function Approach

Hua-Hua Fu,*,† Kai-Lun Yao,*,†,‡ and Zu-Li Liu†,§

Department of Physics, Huazhong University of Science and Technology, Wuhan 430074, China, International Center of Materials Physics, Chinese Academy of Science, Shenyang 110015, China, and State Key Laboratory of Coordination Chemistry, Nanjing University, Nanjing 210093, China

Received: January 20, 2008; Revised Manuscript Received: April 14, 2008

The temperature dependence of magnetic susceptibility and sublattice magnetizations were calculated for a Heisenberg Hamiltonian of an $S = 1$ and $S = {}^1/_2$ antiferromagnetic alternating spin chain by means of the many-body Green's function theory to show the possible occurrence of a ferrimagnetic phase transition for genuinely organic molecule-based magnets. The $S = 1$ site in the chain is composed of two $S = {}^1/_2$ spins coupled by a finite ferromagnetic interaction. From the calculated results, it is found that the sublattice magnetization at low-spin $S = {}^1/_2$ sites changes its sign from negative to positive with increasing temperature, giving rise to the spin alignments along the chain changing from antiferromagnetic to ferromagnetic ones, which indicates that there is a magnetic phase transition occurring. Because of the weak intermolecular antiferromagnetic interactions, the curves of the magnetic susceptibility multiplied by temperature (χT) against temperature show a round peak at low temperatures, which is well consistent with recent experimental observations, and the ferrimagnetic phase transition could only be detected at an ultralow-temperature region and under very weak external magnetic fields in practical organic materials. From the analysis of the sublattice magnetizations, it is uncovered that the appearance of the low-temperature peak in the curves of the χT originates from the ferromagnetic spin alignments for all the spins along the chain, and the intermolecular antiferromagnetic interactions play a pivotal role in ferrimagnetic spin alignments of the magnetic systems. It is also found that the higher spatial symmetry of the intermolecular antiferromagnetic interactions have contributions to stabilize the ferrimagnetic ordering state in the molecule-based magnetic materials.

Introduction

The magnetism of organic molecule-based materials has received great interest both experimentally and theoretically in recent years.[1] Discovery of various organic magnets has given us profound understanding and the development in the fields of materials science and quantum spin mechanics. After the discovery of the first purely organic ferromagnet *p*-NPNN,[2] more than thirty ferromagnets have been well-documented in genuinely organic molecule-based materials. The genuinely organic molecule-based ferrimagnetism has also been attracting much attention, because the organic ferrimagnetism is considered as one of the facile approaches to realize organic magnets. The physical picture of the organic ferrimagnetics has been first proposed theoretically by Buchachenko in 1979.[3] Because of different magnetic moments in the neighboring organic open-shell molecules, the antiferromagnetic interactions between them would bring about antiparallel spin alignments to result in a possible ordered state with net magnetization in the organic assemblages. Shiomi et al. have also presented theoretial consideration in quantum terms on the ferrimagnetic spin alignment in organic molecule-based systems,[4–6] which gives us more evidence-based approaches to the organic ferrimagnetism. However, the magnetic phase transition to an obvious ferrimagnetic ordered state has not been well documented experimentally so far in genuinely organic molecular materials. This presents a remarkable contrast to the investigations on the genuinely organic molecular ferromagnets based on purely ferromagnetic intermolecular interactions[1,2] and transition metal based ferrimagnets.[7] Therefore, to search and to synthesize an organic ferrimagnet is still considered as one of challenging targets in material science.

For experimental crystals, a breakthrough work for this target was made by Izuoka and co-workers in 1994,[8] who synthesized a molecular complex of a ground-state triplet $S = 1$ biradical and $S = {}^1/_2$ monoradical; the mono- and biradical molecules they used are shown as the molecule **1** and molecule **2** in parts a and b of Figure 1, respectively. The complex has exhibited a minimum and an upturnlike behavior in χT below 6 K. This is the first observation of ferrimagnetic behavior in genuinely organic materials. Although the complex has exhibited no long-range ferrimagnetic ordering, it played a pilot role in uncovering a new category of organic magnetics. It is worth noting that Hosokoshi et al.[9] adopted a structure similar to that of Izuoka et al. and have claimed to succeed in making for the first time a genuinely organic molecule-based ferrimagnet by using a single-component strategy. They utilized a triradical including a π biradical with a triplet ($S = 1$) ground-state and a π radical with $S = {}^1/_2$ connected by σ bonds, the $S = 1$ unit is coupled with intramolecular ferromagnetic interactions, and connected with the neighboring $S = {}^1/_2$ unit by intermolecular antiferromagnetic interactions. The triradical molecule is shown as the

* To whom correspondence should be addressed. E-mail: fuhust@yahoo.com.cn (H.-H.F.); klyao@hust.edu.cn (K.-L.Y.).
† Huazhong University of Science and Technology.
‡ Chinese Academy of Science.
§ Nanjing University.

10.1021/jp800554a CCC: $40.75
Published on Web 06/18/2008

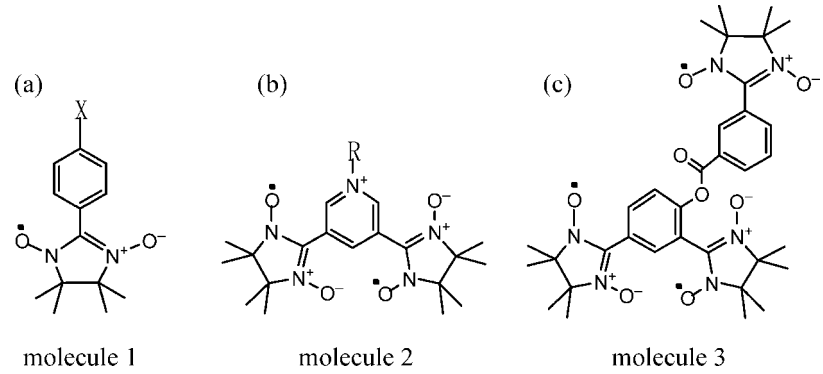

Figure 1. The prototype genuinely organic monoradical molecule **1**, biradical molecule **2**, and triradical molecule **3**, which are used to constitute genuinely organic molecule-based ferrimagnetics.

molecule **3** in Figure 1c. This material undergoes a three-dimensional phase transition as the temperature is cooled down to 0.28 K. By use of a similar single-component strategy, Shiomi et al. achieved another purely organic molecule-based ferrimagnet.[10] From their experiments, the curve of the magnetic susceptibility multiplied by temperature χT against temperature displays as a round peak at about 10 K, and as the temperature is cooled down to 0.28 K, the curve for the product χT shows a minimum and upturnlike behavior, which indicates that a ferrimagnetic spin alignment is achieved in the magnetic systems.

In very recent years, Tanaka et al. proposed a strategy of bioinspired molecular assemblage based on intermolecular hydrogen bonding[11] and achieved a thymine-substituted nitronyl nitroxide biradical as a triplet ($S = 1$) component for the bioinspired ferrimagnetic system. This presents a new idea to design and synthesize genuinely organic molecule-based ferrimagnetics. On the basis of the above-mentioned strategies, Shiomi et al. have devoted to design and synthesize a series of genuinely organic molecule-based ferrimagnetics on experiment.[12] From their magnetic susceptibility measurements, it is found that there is a common characteristic, that is, the curves of the product χT against temperature show a round peak at low temperatures. It is also found that, with decreasing temperature, the χT value increases, indicating that the ferromagnetic interactions are retained in the organic complex; with further decreasing temperature, the χT value drops rapidly, which is attributed to the intermolecular antiferromagnetic interactions along the chain. However, it is regretted that the minimum and upturnlike diverging behavior in the curves of the product χT at low-temperature region, which indicate the possible occurrence of ferrimagnetism, were not observed in these organic materials. Thus, to design and synthesize a genuinely organic molecule-based ferrimagnet with a clear ferrimagnetic phase transition is still a hard task on experiment so far. Under the circumstances, in the present paper, we will explore the possible occurrence of ferrimagnetic phase transition in these purely organic materials and make a clear explanation to the above-mentioned ferromagnetic behaviors in the curves of the product χT on the experimental measurements from a theoretical point of view.

Methods of Computation

In organic molecule-based magnets, spin density is distributed over many atomic sites in an open shell molecule, and hence, the intermolecular spin−spin interaction has a multicentered or multicontact nature.[5,6] Furthermore, in most cases, intramolecular interactions in stable organic $S > {}^1/_2$ molecules are on the same order of magnitude as the intermolecular interactions in crystalline solid states, which indicates that high-spin value $S = 1$ might not be a good quantum number for describing the biradical embedded in the molecular assemblages. Considering these, Shiomi et al. pointed out theoretically that the above-mentioned molecule-based ferrimagnetics should be described as a spin-${}^1/_2$ Heisenberg diamondlike chain model as illustrated in Figure 2.[5,6,13] The Hamiltonian for this model in the presence of an applied static magnetic field B can be written as follows

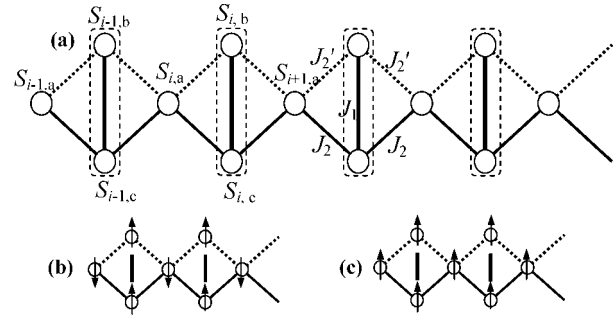

Figure 2. (a), Schematic diagram of a spin-${}^1/_2$ diamondlike spin model. Open circles represent spin-${}^1/_2$ sites, i stands for the superlattice number and unit cell is composed of three subcells $S_{i,a}$, $S_{i,b}$, and $S_{i,c}$ where $S_{i,a}$ indicates a monoradical molecule site, which is coupled with other sites by intermolecular antiferromagnetic interactions J_2 and J_2', and $S_{i,b}$ and $S_{i,c}$ indicate two organic radicals of a biradical sites coupled by intramolecular ferromagnetic exchange interaction J_1. (b) and (c) Two possible spin alignments, ferri- and ferromagnetic states, might occur in the organic magnetic systems.

$$H = \sum_{i}^{N} \Big\{ J_1 S_{i,\mathrm{b}} \cdot S_{i,\mathrm{c}} + J_2 S_{i,\mathrm{a}} \cdot S_{i,\mathrm{c}} + J_2' S_{i,\mathrm{a}} \cdot S_{i,\mathrm{b}} + \frac{1}{2} J_2' (S_{i-1,\mathrm{b}} \cdot S_{i,\mathrm{a}} + S_{i,\mathrm{b}} \cdot S_{i+1,\mathrm{a}}) + \frac{1}{2} J_2 (S_{i-1,\mathrm{c}} \cdot S_{i,\mathrm{a}} + S_{i,\mathrm{c}} \cdot S_{i+1,\mathrm{a}}) + \mathrm{g}\mu_B B (S_{i,\mathrm{a}}^z + S_{i,\mathrm{b}}^z + S_{i,\mathrm{c}}^z) \Big\} \quad (1)$$

where S_j is the spin operator at the jth site, and $S^{\pm} = S^x \pm iS^y$. N is the total number of unit cells in the diamondlike spin chain, and the last term represents the Zeeman energy of the spins with the common g-factor and Bohr magneton μ_B. Here we consider only the case when the external field B is along the z axis direction. It should be noted that, if the model compound is composed of single-component organic triradical molecules, the spin sites $S_{i,a}$, $S_{i,b}$, and $S_{i,c}$ denote the three radicals within a single organic molecule; if the model is a biradical−monoradical alternating chain, the spin sites $S_{i,b}$ and $S_{i,c}$ denote two radicals within a biradical molecule with an intramolecular

ferromagnetic interaction, $J_1(<0)$, and the biradical is coupled with the neighboring monoradical $S_{i,a}$ by intermolecular antiferromagnetic interactions, J_2 and $J_2'(>0)$.

In the practical organic molecule-based assemblages, since there is no strong covalent or electrovalent bonding between two neighboring organic molecules, the intermolecular antiferromagnetic interactions J_2 and J_2' are usually much weaker than the intramolecular ferromagnetic interaction J_1; therefore we will mainly focus on the case J_2 (J_2') < $|J_1|$. It should be pointed out that some numerical studies have been reported mainly by the exact diagonalization method and the quantum Monte Carlo simulations. However, there exists a memory-size limitation for computing in terms of the combination of canonical orthogonalization and Householder diagonalization procedures.[14] And the quantum Monte Carlo simulations are difficult to carry out for very weak intermolecular interactions, because the resultant low T_{min} values prevented numerical covergence in the magnetic susceptibility χ with a satisfactory accuracy.[6] Considering these situations, in the present paper, we will apply the many-body Green's function theory to calculate the magnetic properties of the ferrimagnetic diamondlike spin chains.

The Green's function theory has long been used to treat the Heisenberg exchange model.[15,16] The retarded Green's functions or double-time Green's functions are, according to Bogolyubov and Tyablikov,[17] as follows

$$G_{ij}(t-t') = \langle\langle A_i;B_j\rangle\rangle = -i\theta(t-t')\langle A_iB_j - B_jA_i\rangle \quad (2)$$

where $A_i = S^+_{i,\alpha}, B_j = S^-_{j,\alpha}$ (α = a, b, and c) and the subscripts i and j label lattice sites. The Green's function is Fourier time transformed and then put into the equation of motion

$$\omega\langle\langle A_i;B_j\rangle\rangle = \frac{1}{2\pi}\langle[A_i, B_j]\rangle + \langle\langle[A_i, H];B_j\rangle\rangle \quad (3)$$

Higher-order Green's functions are decoupled by the random phase approximation such as $\langle\langle S^z_iS^+_i;S^-_j\rangle\rangle = \langle S^z_i\rangle\langle\langle S^+_i;S^-_j\rangle\rangle (i'\neq i)$. By the commutator of $S^+_{i,\alpha}$ and the Hamiltonian, one can obtain the linear equations

$$\sum_{\lambda=1}^{L}[\omega(k)\delta_{\mu\lambda} - P_{\mu\lambda}(k)]g_{\lambda\nu}(\omega,k) = \frac{\delta_{\mu\nu}}{2\pi}\langle[S^+_\mu, S^-_\nu]\rangle \quad (4)$$

The order of parameter matrix P in above formula is three,[18] which is due to the fact that every crystal cell contains three sublattices, e.g., the sublattice a, b, and c. From the above formula, the Green's function $g_{\lambda\nu}$ in the k-space can be obtained. According to the well-known spectral theorem, the statistical average of the product of the operators can be calculated as

$$\langle B_jA_i\rangle = \frac{i}{2\pi N}\sum_k e^{ik\cdot(i-j)}\int\frac{d\omega}{e^{\beta\omega}-1}[g(\omega+i0^+,k) - g(\omega-i0^+,k)] \quad (5)$$

Considering the spin value of $S = {}^1/_2$ in the ferrimagnetic diamondlike chain, the statistical averages of the sublattice magnetizations $\langle S^z_\alpha\rangle$ (α = a, b, c) can be evaluated by the formula $\langle S^z_\alpha\rangle = {}^1/_2 - \langle S^-_\alpha S^+_\alpha\rangle$ (α = a, b, and c). Then the average magnetization in every repeating cell M_{tot} and the magnetic susceptibility χ are defined as

$$\langle M_{tot}\rangle = \frac{1}{N}\sum_i^N(\langle S^z_{i,a}\rangle + \langle S^z_{i,b}\rangle + \langle S^z_{i,c}\rangle), \chi = \frac{\partial\langle M_{tot}\rangle}{\partial B} \quad (6)$$

These equations must be calculated self-consistently,[19] and then the magnetizations, the magnetic susceptibility, and other magnetic properties can be achieved.

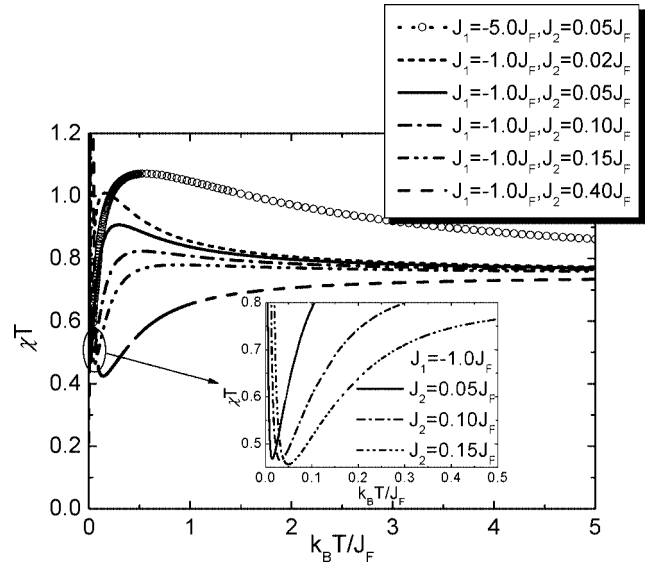

Figure 3. Temperature dependence of the product χT of the magnetic systems for the symmetric Hamiltonian case ($J_2 = J_2'$). The magnetic coupling parameters are set as $J_2 = 0.05J_F$ for $J_1 = -5.0J_F$ and $J_2 =$ 0.02, 0.05, 0.10, 0.15, and $0.4J_F$ for $J_1 = -J_F$ from top to down. In the inset is the low-temperature part of the plotted χT against temperature.

Results and Discussion

1. Symmetric Ferrimagnetic Diamondlike Spin Chains. First we consider the symmetric Hamiltonian case, where all intermolecular antiferromagnetic interactions are uniform ($J_2 = J_2'$). The temperature dependence of the magnetic susceptibility multiplied by temperature is illustrated in Figure 3 at the external magnetic field $B = 0.002J_F/g\mu_B$. The magnetic coupling parameters are set as $J_2 = 0.05J_F$ for $J_1 = -5.0J_F$, and $J_2 =$ 0.02, 0.05, 0.10, 0.15, and $0.4J_F$ for $J_1 = -J_F$. In order to obtain comparable numerical results, we take J_F as the magnetic exchange interaction unit (can be considered as 1). From the figure, it can be seen that, for $J_2 \ll |J_1|$ and $J_1 = -J_F$, the χT value increases as the temperature is lowered, which indicates the existence of ferromagnetic exchange interactions within the organic complex. With further decreasing temperature, the χT value increases to a maximum and then drops rapidly, which gives rise to the curves of the product χT against temperature showing as a round peak at low temperatures. This phenomenon is well consistent with the recent experimental observations on some genuinely organic molecule-based ferrimagnetics.[11,12,20] It is clear that the peak is very sensitive to the changing of the intermolecular antiferromangnetic interactions J_2 and J_2'. With increasing of J_2 and J_2', the peak is suppressed and moves toward higher temperature region. However, the intramolecular ferromagnetic interaction only makes the curve of χT move up with little influence on the peak (see the circle curve for $J_1 = -5.0J_F$, $J_2 = 0.05J_F$ in Figure 3). It is interesting that, as the temperature is cooled down to the ultra-low-temperature region for $k_BT/J_F < 0.1$, the curves of the product χT against temperature shows a minimum and upturnlike behavior (see the curves labeled as $J_2 = 0.05$, 0.10, and $0.15J_F$ in the inset of Figure 3), which is indicative of the ferrimagnetic-like behavior in low-dimensional lattices. The low-temperature limit of the χT diverges, suggesting the possible occurrence of ferrimagnetism in the magnetic systems. It should be pointed out that the magnetic susceptibility measurement for a purely organic molecule-based ferrimagnet by Shiomi et al.[10] just testifies our theoretical results. On their experiments, the round peak in the

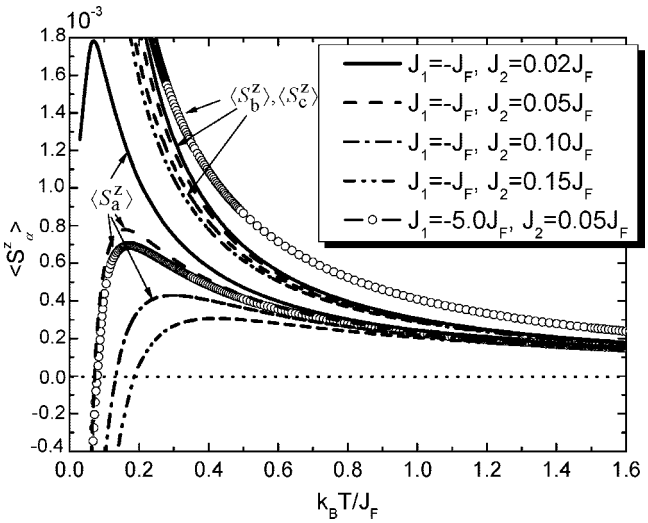

Figure 4. Temperature dependence of the sublattice magnetizations $\langle S_\alpha^z \rangle$ (α = a, b, and c) of the magnetic systems for the symmetrical Hamiltonian case. The magnetic coupling parameters are set as J_2 = 0.02, 0.05, 0.10, and $0.15J_F$ for $J_1 = -J_F$ and $J_2 = 0.05J_F$ for $J_1 = -5.0J_F$ (line with circles).

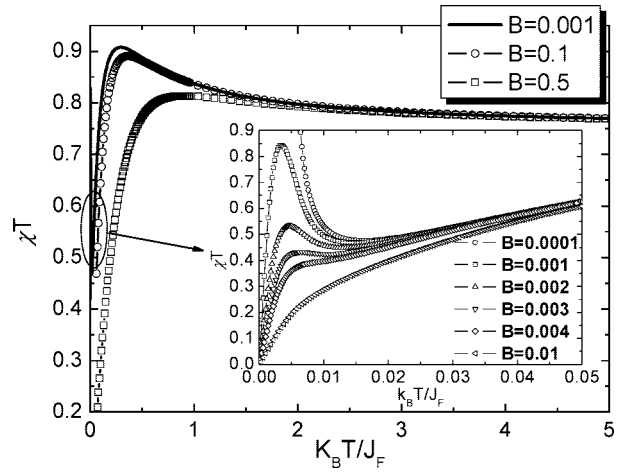

Figure 5. Temperature dependence of the product χT for the symmetric Hamiltonian case in different external magnetic fields for B = 0.001, 0.1 and $0.5J_F/g\mu_B$. In the inset is the low-temperature part of the χT against temperature, the external magnetic field B is set as 0.0001, 0.001, 0.002, 0.003, 0.004, and $0.01J_F/g\mu_B$.

curve of the χT is located at about 10 K, and when the temperature is cooled down until to 0.28 K, the minimum in the curve of the χT is detected. With further decreasing temperature, the curve of the χT shows an upturnlike behavior, which is consistent with our numerical results. From the inset of Figure 3, it is also uncovered that, with increasing of the intermolecular antiferromagnetic interactions J_2 and J_2', the minimum decreases and moves toward higher temperatures, and the upturnlike diverging behavior becomes more and more clear. So it is concluded that the intermolecular antiferromagnetic interactions play an important role in the formation of these ferrimagnetic ordered state in the purely organic molecule-based materials.

To further investigate the appearance of the low-temperature peak in the curves of the product χT against temperature, the corresponding temperature dependence of the sublattice magnetizations $\langle S_\alpha^z \rangle$ (α = a, b, and c) are presented in Figure 4. From the figure, it is clear that $\langle S_a^z \rangle < 0$ and $\langle S_{b,c}^z \rangle > 0$ at very low temperatures, indicating that the antiferromagnetic spin alignments occur as shown in Figure 2b. With increasing temperature, the sublattice magnetization $\langle S_a^z \rangle$ changes its sign from negative to positive, which gives rise to a compensation temperature T_{comp} appearing in the curves of the sublattice magnetization $\langle S_a^z \rangle$ against temperature. As a result, all the spins along the chain display as ferromagnetic spin alignments as shown in Figure 2c above the temperature T_{comp}. These magnetic phenomena can be explained as follows. In fact, a small external magnetic field is applied to the magnetic systems, and the external field will open up an energy gap. Thus there is a competition between the intermolecular antiferromagnetic interactions and the external magnetic fields. As the temperature ascends, the thermal fluctuation destroys the antiferromagnetic ordering and makes the influence of the external fields which makes all the spins point to one direction become more and more dominant. It is also found that, with further increasing temperature, the curves of the $\langle S_a^z \rangle$ show a round peak and then decrease, indicating that the thermal fluctuation strengthens the sublattice magnetization $\langle S_a^z \rangle$. And with increasing intermolecular antiferromagnetic interactions $J_2(J_2')$, the compensation temperature T_{comp} ascends; at the same time, the round peak is suppressed and shifts toward higher temperature region. This changing trendery is similar to that of the low-temperature peak in the curves of the product χT. However, the strengthening of the intramolecular ferromagnetic interaction J_1 seems to have little influence on $\langle S_a^z \rangle$ (see the curve for $J_1 = -5.0J_F$, $J_2 = 0.05J_F$ in Figure 4), which indicates that the low-temperature magnetic properties are governed by the intermolecular antiferromagnetic interactions. Nevertheless, these interesting behaviors on the $\langle S_a^z \rangle$ do not occur on the sublattice magnetizations $\langle S_b^z \rangle$ and $\langle S_c^z \rangle$. Recalling Figure 3, we can find that the low-temperature peaks in the curve of the χT are just located at the corresponding ferromagnetic phase as shown in Figure 4. So it is concluded that the ferromagnetic behaviors on the curves of the χT originate from the ferromagnetic spin alignments for all the spins along the chain, which clarifies the past explanation that the ferromagnetic behaviors are only attributed to the intramolecular ferromagnetic interactions.

The influence of the external magnetic fields on the magnetic properties of the magnetic systems is also calculated; the numerical results are illustrated in Figure 5. It is obvious that stronger external fields make the low-temperature peak suppressed and move toward higher temperature region. At high-temperature region, the influence of the external fields can be neglected, because the system is just in a paramagnetic phase. In particular, we should turn our attention to the ultralow-temperature region for $k_BT/J_F < 0.03$, where the influence of the external fields on the magnetic properties is subtle as shown in the inset of Figure 5. When the external field is qutie small ($B = 0.0001J_F/g\mu_B$ as seen in the inset of Figure 5), the low-temperature limit of the χT diverges, which is similar to the discussions before; as the external field increases to a larger value, the curve for the χT emerges a sharp peak at low temperatures, indicating that the external field opens up an energy gap, which makes the χT value go exponentially to zero for the temperature less than the gap in the applied field. With further increasing of the external field, the peak is suppressed and shifts toward high-temperature region. However, as the external field B increases up to about $0.004J_F/g\mu_B$, the low-temperature peak and the minimum at intermediate temperatures both vanish. So it is concluded that, only under very low external fields, the minimum and upturnlike behavior in the curves of the χT against temperature could be detected in the genuinely organic molecule-based ferrimagnetics with weak intermolecular antiferromagnetic interactions.

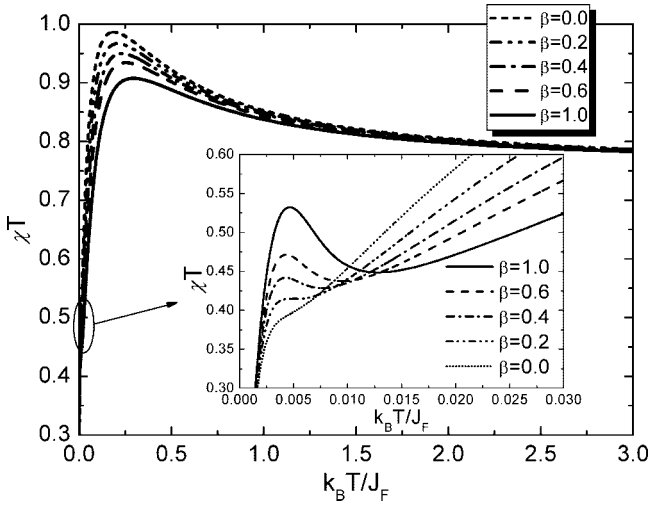

Figure 6. The temperature dependence of the product χT of the magnetic systems for the unsymmetrical Hamiltonian case at the external field $B = 0.002J_F/g\mu_B$. The magnetic coupling parameters are set as $J_1 = -J_F$, the ratio $\beta = J_2'/J_2$ signifying the spatial symmetry degree of the intermolecular antiferromagnetic interactions, and is set as 0.0, 0.2, 0.4, 0.6, and 1.0. In the inset is the low-temperature part of the plotted χT against temperature.

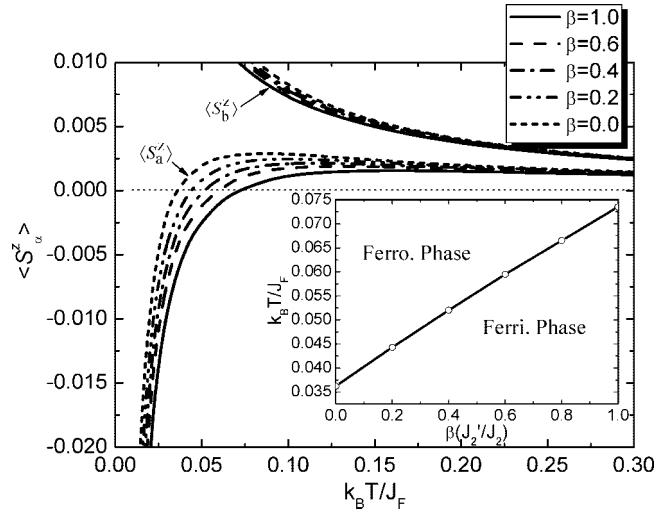

Figure 7. Temperature dependence of the sublattice magnetizations $\langle S_\alpha^z \rangle$ (α = a, b, and c) for the unsymmetrical Hamiltonian case at the external field $B = 0.002J_F/g\mu_B$. The magnetic coupling parameters are set as $J_1 = -J_F$, the ratio $\alpha = J_2'/J_2$ signifying the spatial symmetry degree of the intermolecular antiferromagnetic interactions, and is set as 0.0, 0.2, 0.4, 0.6, and 1.0. In the inset is the $T-\beta$ phase diagram for this case.

2. Unsymmetrical Ferrimagnetic Diamondlike Spin Chains. For an organic molecule-based magnet, the intermolecular interactions have a multicentered nature and a low spatial symmetry. So it is essential to discuss the influence of the spatial symmetry lowering of the intermolecular antiferromagnetic interactions on the spin distribution of the spin chain. The temperature dependence of the product χT for this case at the external magnetic field $B = 0.002J_F/g\mu_B$ is illustrated in Figure 6. The parameters are set as $J_1 = -J_F$, $J_2 = 0.05J_F$, and $J_2' = \beta J_2$, where the parameter ratio α signifies the spatial symmetry degree of the intermolecular antiferromagnetic exchange interactions. From the figure, it can be seen that, as the spatial symmetry of the intermolecular interactions is lowered, e.g., the parameter ratio β decreases, the low-temperature peak in the curves of the product χT against temperature moves toward the lower-temperature region and its maximum increases, indicating the strengthening of its ferromagnetic behaviors within the spin chain. It should be stressed that the minimum and upturnlike behavior, which are characteristic of the occurrence of the ferrimagnetic ordered state of the magnetic systems, are also achieved as shown in the inset of Figure 6 in the ultra-low-temperature region for $k_BT/J_F < 0.02$. In the inset figure, the appearance of the low-temperature peak is attributed to the external magnetic field as discussed obove. It is found that, as the spatial symmetry parameter ratio β is lowered, the minimum of the curve for the χT decreases and moves toward lower temperature region; as the parameter ratio β decreases to 0.2, the minimum and the peak both vanish, indicating that the ferrimagnetic ordered state could not be detected in this case. So it is concluded that the higher spatial symmetry of the intermolecular antiferromagnetic interactions has contributions to form and to stabilize the ferrimagnetic ordered state in the organic materials.

The corresponding sublattice magnetizations $\langle S_\alpha^z \rangle$ against temperature for the unsymmetrical Hamiltonian case are also considered, and the numerical results are presented in Figure 7. From Figure 7, one can see that, with increasing of the spatial symmetry parameter ratio β, the low-temperature round peak in the curves of the $\langle S_a^z \rangle$ is suppressed and moves toward higher temperature region, giving rise to the compensation temperature T_{comp} in the curve of $\langle S_a^z \rangle$ ascending. From the above analysis for the sublattice magnetizations, we can obtain the $T-\beta$ phase diagram as shown in the inset of Figure 7. From the phase diagram, we can find that the magnetic phase transition temperature increases linearly with the increasing of the spatial symmetry parameter ratio β. So it can be believed that higher spatial symmetry of the intermolecular exchange interactions and the lowering temperatures have contributions to the occurrence of ferrimagnetic spin alignments along the chain.

Conclusion

The ferrimagnetic ordering in the genuinely organic molecule-based quantum diamondlike spin chains have theoretically been studied by means of the many-body Green's function theory within the random phase approximation. Because of the very weak intermolecular antiferromagnetic interactions, the curves of the product χT against temperature show as a round peak at low temperature region, which is consistent with the very recent experimental observations. The minimum and low-temperature upturnlike diverging behavior in the curves of the χT, which is indicative of the occurrence of the ferrimagnetic phase transition of the system, could only be detected at an ultra-low-temperature region. From the synthesis of the sublattice magnetizations, the appearance of the low-temperature peak in the curves of the product χT originates from the ferromagnetic spin alignments for all the spins along the chain. It is concluded that the intermolecular antiferromagnetic interactions play an important role in the formation of the ferrimagnetic ordered state in the magnetic systems. It is also uncovered that the higher spatial symmetry has contributions to the formation of the ferrimagnetic spin alignments of the magnetic systems. Therefore, the strengthening of the intermolecular antiferromagnetic interactions and the higher spatial symmetry of the intermolecular exchange interactions are necessary to accomplish the ferrimagnetic spin alignments at higher temperature region in practical genuinely organic molecule-based magnets.

Acknowledgment. This work was supported by the National Natural Science Foundation of China under Grant Nos. 10574047,

10574048, and 10774051. This work was also supported by the National 973 Project under Grant. No 2006CB921605.

References and Notes

(1) (a) Rajca, A.; Wongsriratanakul, J.; Rajca, S. *Science* **2001**, *294*, 1503. (b) Rajca, A.; Rajca, S.; Wongsriratanakul, *J. Am. Chem. Soc.* **1999**, *121*, 6308. (c) Wang, W. Z.; Yao, K. L.; Lin, H. Q. *Chem. Phys. Lett.* **1997**, *274*, 221. (d) Wang, W. Z.; Yao, K. L.; Lin, H. Q. *J. Chem. Phys.* **1998**, *108*, 2867. (e) Takeda, K.; Yoshida, Y.; Inanaga, Y.; Kawae, T.; Shiomi, D.; Ise, T.; Kozaki, M.; Okada, K.; Sato, K.; Takui, T. *Phys. Rev. B* **2005**, *72*, 024435. (f) Hayakawa, K.; Shiomi, D.; Ise, T.; Sato, K.; Takui, T. *J. Phys. Chem. B* **2005**, *109*, 9195. (g) Maekawa, K.; Shiomi, D.; Ise, T.; Sato, K.; Takui, T. *J. Phys. Chem. B* **2005**, *109*, 9299. (h) Murata, H.; Mague, J. T.; Aboaku, S.; Yoshioka, N.; Lahti, P. M. *Chem. Mater.* **2007**, *19*, 4111.

(2) (a) Tamura, M.; Nakazawa, Y.; Shiomi, D.; Nozawa, K.; Hosokoshi, Y.; Ishikawa, M.; Takahashi, M.; Kinoshita, M. *Chem. Phys. Lett.* **1991**, *186*, 401. (b) Takahashi, Y.; Tamura, M.; Shirakawa, M.; Shiomi, D.; Takahashi, M.; Kinoshita, M.; Ishikawa, M. *Phys. Rev. B* **1992**, *46*, 8906.

(3) Buchachenko, A. L. *Dokl. Akad. Nauk.* **1979**, *244*, 107.

(4) Shiomi, D.; Sato, K.; Takui, T. *J. Phys. Chem. B* **2000**, *104*, 1961.

(5) Shiomi, D.; Sato, K.; Takui, T. *J. Phys. Chem. B* **2001**, *105*, 2932.

(6) Shiomi, D.; Sato, K.; Takui, T. *J. Phys. Chem. A* **2002**, *106*, 2096.

(7) For examples, see: (a) Kahn, O.; Pei, Y.; Verdaguer, M.; Renard, J. P.; Sletten, J. *J. Am. Chem. Soc.* **1988**, *110*, 782. (b) Caneschi, A.; Gatteschi, D.; Renard, J. P.; Rey, P.; Sessoli, R. *Inorg. Chem.* **1989**, *28*, 1976.

(8) (a) Izuoka, A.; Fukada, M.; Kumai, R.; Itakura, M.; Hikami, S.; Sugawara, T. *J. Am. Chem. Soc.* **1994**, *116*, 2609. (b) Izuoka, A.; Fukada, M.; Sugawara, T. *Mol. Cryst. Liq. Cryst.* **1993**, *232*, 103.

(9) (a) Hosokoshi, Y.; Katoh, K.; Nakazawa, Y.; Nakano, H.; Inoue, K. *J. Am. Chem. Soc.* **2001**, *123*, 7921. (b) Hosokoshi, Y.; Katoh, K.; Inona, K. *Synth. Met.* **2003**, *133*, 527.

(10) Shiomi, D.; Kanaya, T.; Sato, K.; Mito, M.; Takeda, K.; Takui, T. *J. Am. Chem. Soc.* **2001**, *123*, 11823.

(11) Tanaka, H.; Shiomi, D.; Ise, T.; Sato, K.; Takui, T. *Polyhedron* **2007**, *26*, 2230.

(12) (a) Hayakawa, K.; Ise, T.; Shiomi, D.; Sato, K.; Takui, T. *Polyhedron* **2007**, *26*, 1885. (b) Maekawa, K.; Ise, T.; Shiomi, D.; Sato, K.; Takui, T. *Polyhedron* **2007**, *26*, 2347. (c) Kanzaki, Y.; Shiomi, D.; Ise, T.; Sato, K.; Takui, T. *Polyhedron* **2007**, *26*, 1901. (d) Maekawa, K.; Shiomi, D.; Ise, T.; Sato, K.; Takui, T. *J. Phys. Chem. B* **2005**, *109*, 3303. (e) Ise, T.; Shiomi, D.; Sato, K.; Takui, T. *Synth. Met.* **2005**, *154*, 297. (f) Kaneda, C.; Shiomi, D.; Sato, K.; Takui, T. *Polyhedron* **2003**, *22*, 1809.

(13) Nishizawa, M.; Shiomi, D.; Sato, K.; Takui, T.; Itoh, K.; Sawa, H.; Kato, R.; Sakurai, H.; Izuoka, A.; Sugawara, T. *J. Phys. Chem. B* **2000**, *104*, 503.

(14) Shiomi, D.; Nishizawa, M.; Sato, K.; Takui, T.; Itoh, K.; Sakurai, H.; Izuoka, A.; Sugawara, T. *J. Phys. Chem. B* **1997**, *101*, 3342.

(15) Bogolyubov, N. B.; Tyablikov, S. V. *Sov. Phys. Dokl.* **1959**, *4*, 589.

(16) (a) Fu, H. H.; Yao, K. L.; Liu, Z. L. *Phys. Rev. B* **2006**, *73*, 104454. (b) Fu, H. H.; Yao, K. L.; Liu, Z. L. *Phys. Lett. A* **2006**, *358*, 443. (c) Fu, H. H.; Yao, K. L.; Liu, Z. L. *J. Chem. Phys* **2008**, *128*, 114705.

(17) (a) Tyablikov, S. V. *Method in the Quantum Theory of Magnetism*; Plenum: New York, 1967. (b) Callen, H. B. *Phys. Rev.* **1963**, *130*, 890. (c) Wang, H. Y.; Chen, K. Q.; Wang, E. G. *Phys. Rev. B* **2002**, *66*, 092405.

(18) The formula of the matrix P can be written in detail as follows: $P_{11} = -(g\mu_B B + 2.0J_2'\langle S_b^z\rangle + 2.0J_2\langle S_c^z\rangle)$, $P_{12} = J_2'\langle S_a^z\rangle\gamma_k$, $P_{13} = J_2\langle S_a^z\rangle\gamma_k$, $P_{21} = J_2'\langle S_b^z\rangle\gamma_k^*$, $P_{22} = -(g\mu_B B + 2.0J_2'\langle S_a^z\rangle + J_1\langle S_c^z\rangle)$, $P_{23} = J_1\langle S_b^z\rangle$, $P_{31} = J_2\langle S_c^z\rangle\gamma_k^*$, $P_{32} = J_1\langle S_c^z\rangle$, $P_{33} = -(g\mu_B B + 2.0J_2\langle S_a^z\rangle + J_1\langle S_b^z\rangle)$, where $\gamma_k = 1 + e^{ik}$ and k represents the wavevector.

(19) In calculation, an initial state, composed by a set of magnetizaitions $\{\langle S_\alpha^z\rangle\}$, is put into the equations to produce the resultant magnetizations. The iteration goes on until convergence is reached.

(20) (a) Kanaya, T.; Shiomi, K.; Sato, K.; Takui, T. *Polyhedron* **2001**, *20*, 1397. (b) Shiomi, D.; Nishizawa, M.; Kamiyama, K.; Hase, S.; Kanaya, T.; Sato, K.; Takui, T. *Synth. Met.* **2001**, *121*, 1810.

JP800554A